Polymer Bulletin 40, 305–311 (1998)

Polymer Bulletin

Temperature-dependent fracture mechanisms in gel-spun hot-drawn ultra-high molecular weight polyethylene fibres

D. J. Dijkstra[1], E. Pras[2], A. J. Pennings[2]

[1] Bayer AG, Central R & D Department, D-51368 Leverkusen, Germany
[2] Department of Polymer Chemistry, Groningen University, Nijenborgh 4, 9747 AG Groningen, The Netherlands

Received: 10 October 1997/Accepted: 31 October 1997

Summary

Tensile testing of gel-spun hot-drawn ultra-high molecular weight polyethylene (UHMWPE) fibres reveal a ductile-brittle transition temperature. Ductile fracture above the transition temperature is believed to be initiated by a stress-induced orthorhombic-hexagonal phase transition, whereas at lower temperatures brittle fracture occurs in the orthorhombic phase. SEM micrographs of the fracture surfaces of UHMWPE fibres fractured below the transition temperature show fibrillar fracture and cannot be distinguished from fibres fractured in a ductile way above the transition temperature.

Introduction

The experimentally determined tensile strength and modulus of gel-spun hot-drawn UHMWPE fibres has fascinated many investigators. Various theoretical and empirical models have been introduced in an attempt to describe the material properties of these highly oriented, highly crystalline fibres. In some of the models, the properties of the crystalline phase are used to predict the ultimate tensile strength (1). Other models assume the irrelevance of the molecular architecture and morphology and explain the mechanical properties by the draw ratio dependent orientation of the polymer (3). In a third set of models, morphological characteristics are explicitly taken into account (4).

It is the purpose of the present paper to provide further evidence for the role of the orthorhombic-hexagonal phase transition in the temperature dependent tensile strength of gel-spun hot-drawn UHMWPE fibres. The fracture surface of brittle and ductile fractured fibres was studied in order to investigate the temperature dependent fracture mechanisms of these highly fibrillar structures.

Experimental

The UHMWPE used in this study was Hercules Hifax 1900 (Mw=5.5 10^6, Mn= 2 10^6 kg/kmol). The Hifax powder 1.5% by wt. and 0.5% by wt. antioxidant (Ionol from Aldrich, 2,6-di-tert-butyl-4-methylphenol) were added to paraffin oil at 120 °C. Then,

under continuous stirring, the suspension was slowly heated to 150 °C. The gel was kept at 150 °C under a nitrogen atmosphere. Subsequently the solution was allowed to form a gel by slow cooling to room temperature.
Spinning was performed in a cylinder-piston apparatus with a 0.5 mm conical die at 190 °C without stretching.
Prior to hot-drawing, the paraffin-oil was extracted from the gel-filaments in n-hexane for 2 days. The extracted filaments were vacuum dried at 50 °C for one hour. Hot-drawing was carried out at 148 °C in an electrically heated open-ended cylinder oven, 23 cm in length. The velocity of the undrawn fibre at the entrance to the oven was 6 mm/min. Fibre A was hot-drawn in one step to a draw ratio of $\lambda = 50$. Fibre B in two steps to a draw ratio of $\lambda = 200$.
The mechanical testing was performed in a tensile tester at a cross-head speed of 20.6 mm/min and an original sample length of 45 to 60 mm. The cross-sectional areas of the fibres were determined from fibre weight and length assuming a density of 1000 kg/m^3.

Scanning electron microscopy was performed with an Jeol 6320 FESEM microscope operating at 5 kV. The samples were covered with a 2 nm thick layer of gold by sputtering.

Results

The temperature dependent tensile strength of the ultra-high strength polyethylene fibres is shown in Fig. 1 for sample A ($\lambda = 50$) and Fig. 2 for sample B ($\lambda = 200$). Above room temperature, a linear decrease of the tensile strength with increasing temperature is found.Extrapolation to zero tensile strength yields a temperature of about 150 °C, almost exactly the temperature known to be the orthorhombic-hexagonal phase transition

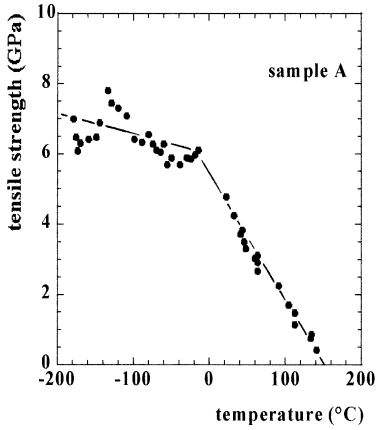

Fig. 1 Tensile strength versus testing temperature (Sample A)

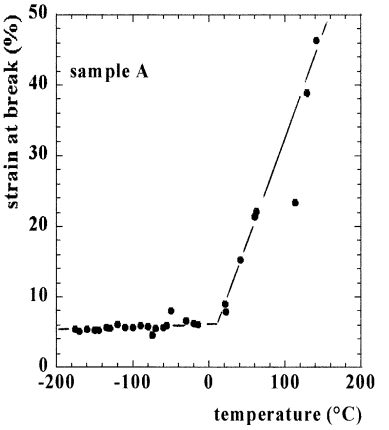

Fig. 2 Elongation at break versus testing temperature (Sample A)

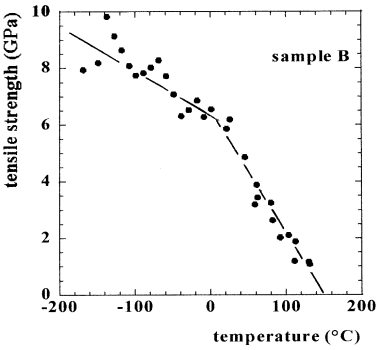

Fig. 3 Tensile strength versus testing temperature (Sample B)

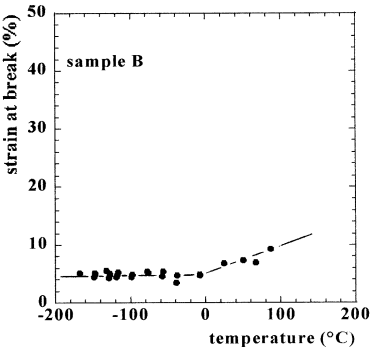

Fig. 4 Elongation at break versus testing temperature (Sample B)

temperature (T_{oh}) for constrained UHMWPE fibres (5). At temperatures below 0 °C, a less pronounced temperature dependence was found. As described in (6), the tensile strength in the low-temperature regime is thought to be determined by the rupture of covalent bonds, whereas at temperatures above 0 °C, the temperature dependent tensile strength of gel-spun hot-drawn UHMWPE fibres is explained by a stress-induced orthorhombic-hexagonal phase transition.

The transition temperature from ductile to brittle fracture can be seen even more clearly in the strain-temperature plot (Fig. 3, Fig. 4). The tensile strain at break at the low temperature regime is about 0.05, whereas the strain at break in the high temperature regime is a strongly increasing function with the temperature. The temperature dependent tensile properties of these fibres with a tensile strength at room temperature of up to 6 GPa confirm those in reference (6) on gel-spun hot-drawn UHMWPE fibres with a tensile strength at room temperature of only 4 GPa. Due to the low strain at break and the almost perfect Hookian stress-strain dependence up to break (5, 7), the fracture surface of the fibres in the low temperature regime was expected to have a brittle appearance. Fig. 5 and Fig. 6 show that the fibres broken at -160 °C and -10 °C still exhibit tapered fibre ends. In contrast to e.g. UHMWPE fibres highly cross-linked by electron beam radiation (8) or dicumylperoxide (9), where brittle failure was accompanied by a smooth non-tapered fracture surface, the fibres in the present study showed highly fibrillar fracture in the tensile testing temperature range from -180 °C up to the constrained melting temperature of 152 °C. Fibres broken at higher temperatures show a high degree of recoiling of the tapered fibre ends, as shown in Fig. 7 for a fibre tested at 60 °C.

Discussion

In semicrystalline polymers two different kinds of morphological textures can be seen. Folded chain crystals (FCC), first studied by Keller (10), and extended chain crystals

Fig. 5

SEM micrograph of the fibre end of a fibre tested at T = -160 °C

⊢⊣ 10µm

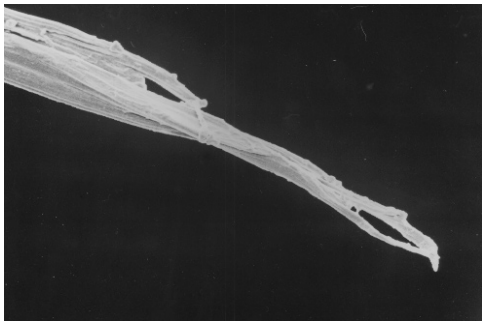

Fig. 6

SEM micrograph of the fibre end of a fibre tested at T = -10°C

⊢⊣ 10µm

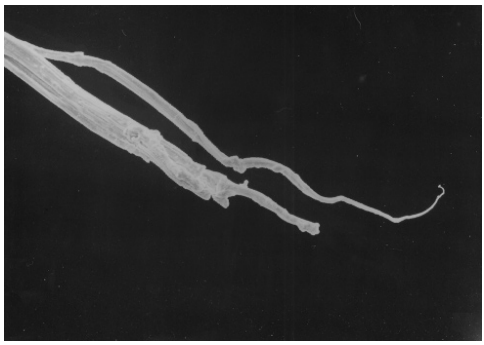

Fig. 7

SEM micrograph of the fibre end of a fibre tested at T = + 60°C

⊢⊣ 10µm

(ECC) first published by Wunderlich (11). Bassett *et al*. (12) suggested, on the basis of thermal analysis and X-ray investigations on polyethylene under high pressure, that crystallisation into the orthorhombic structure gives the FCC morphology and that crystallisation into the hexagonal phase gives the ECC structure. An excellent review on crystallisation and melting of polyethylene has recently been published by Hoffman and Miller (13).

Pechhold (14) describes the melting of polymers to be at least a two-step transition. First, an intermediate phase called the condis (conformational disordered) phase after Wunderlich and secondly, the melting of this condis phase by co-operative formation of dislocations, comparable to the melting of atomic crystals (15). For polyethylene at atmospheric pressure both transitions coincide in one transition from the orthorhombic crystal to the isotropic melt. For pressures above 350 Mpa polyethylene exhibits two transitions: the first step transforms the all-trans crystal in a 'quasi-hexagonal' or columnar phase (16), which is considered as a cylindrical packing of conformational disordered chains. The orthorhombic, hexagonal and melt phases at high pressures are shown in the phase diagram in Fig. 8 (17).
The first derivative of the solid-melt transition temperature versus pressure curve at atmospheric pressure is non-zero (see Fig. 8 (17)), an indication that a decreasing transition temperature at even lower pressures is to be expected. The hydrostatic pressure is the summation of the three principal stresses: $p = - 1/3(\sigma_1+\sigma_2+\sigma_3)$. For uniaxial tensile

Fig. 8

Equilibrium phase diagram of polyethylene obtained from dilatometric (open symbols) and mechanical (filled symbols) investigations (after (17)

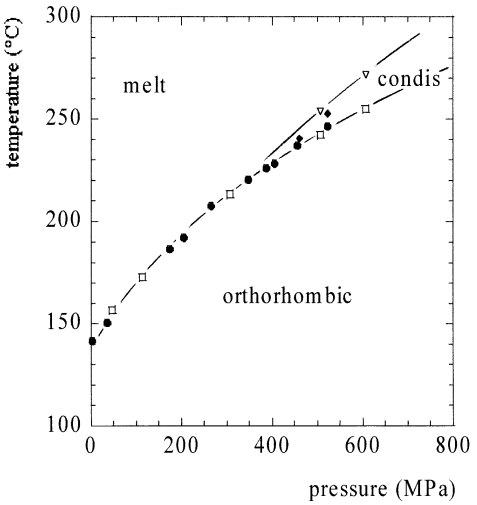

deformation $\sigma_2 = 0$ and $\sigma 3 = 0$, that is the hydrostatic pressure in fibres is directly proportional to the tensile stress: $p = - 1/3\ \sigma_1$

The hierachical morphology of UHMWPE fibres consists of macrofibrils and microfibrils (18, 19). The crystal structure of the microfibrils is believed to be an ECC-like morphology with small disordered domains, which still include an enhanced fraction of all-trans sequences (2), containing imperfections like entanglements, chain ends, folds, etc. (4). Cantow et al. (19) found by atomic force microscopy under water on the fibril surface a long period of about 10 to 20 nm, that was assigned to sequences of crystalline and less-

ordered regions. Highly strained taut-tie molecules transfer the stress from one ECC domain into the other (20).

A stress induced orthorhombic-hexagonal phase transition has been used (6, 21) to explain the linear decrease in tensile strength of gel-spun hot-drawn UHMWPE fibres above room temperature. Smith (22) calculated the theoretical strength of a perfect PE fibre at room temperature to be 7 to 9 GPa, by treating it as a stressed crystal undergoing an (orthorhombic) crystal-melt phase transition. Yamamoto *et al*. (23) showed that interchain coherence in the hexagonal crystal is very weak compared to that in the orthorhombic crystal. In locally highly stressed crystalline domains (24, 25), the orthorhombic-hexagonal phase transforms into the hexagonal phase, and the chains can easily slip past one another, thereby relieving the locally high stresses. Due to the reduction in local stress the hexagonal phase transforms back to the orthorhombic phase.

The orthorhombic-hexagonal phase transition in UHMWPE fibres has been confirmed by real-time X-ray diffraction measurements on constrained samples (26, 27). Temperature dependent WAXS on cross-linked UHMWPE fibres (5) showed that the inter-chain cross-links in the disordered domains prevent extensive chain slippage and thereby fibre failure.

The tapered fibrillar fracture fibre ends at temperatures below T_{oh}, as shown in Fig. 5-6, indicate that fracture of an UHMWPE monofilament can be imagined as the fracture of a bundle of separate macrofibrils, where the fracture ends of each macrofibril do not necessarily lie in one plane. The influence of fibre diameter, i.e. the number of macrofibrils in the cross-section of the monofilament, on the tensile strength of UHMWPE fibres as found in (28) can be explained by a more efficiently developed orientation of the macrofibrils by drawing thinner fibres (29).

References

1. Peterlin A (1979) In: Chifferi A, Ward IM (ed) Ultra-high modulus polymers, Applied Science Publishers Ltd, England pp 279
2. Strobl G (1996) The Physics of Polymers, Springer
3. Dirix Y, Tervoort TA, Bastiaansen CWM, Lemstra PJ (1995) J. Text. Inst. 86:314
4. Dijkstra DJ, Pennings AJ (1988) Polym. Bull. 19: 73
5. Torfs JCM (1983) PhD thesis, University of Groningen, The Netherlands
6. Dijkstra DJ, Torfs JCM, Pennings AJ (1989) Coll. Polym. Sci.267: 866
7. Van der Werff H, Pennings AJ (1991) 269:747
8. Dijkstra DJ, Pennings AJ (1987) Polym. Bull. 17:507
9. De Boer J, Pennings AJ (1981) Polym. Bull. 5: 317
10. Keller A, Phil. Mag. (1957) 2:1171
11. Wunderlich B, Arakawa T (1964) J. Polym. Sci. 2: 3697
12. Bassett DC, Block S, Piermarini GJ (1974) J. Appl. Phys. 45: 4146
13. Hoffman JD, Miller RL (1997) Polymer 38: 3151
14. Pechhold W (1991) Polymers under pressure.In: Hochheimer HD, Etters RD (ed) Frontiers of High-Pressure Research, Plenum Press, New York, pp. 1
15. Pechhold W, Groβmann HP, W. v. Soden, Coll. Polymer Sci. (1982) 260: 248
16. Ungar G (1993) Polymer 34:2050
17. Theobald S, Pechhold W, (1994) High Pressure in Material Science and Geoscience XXXII Annual Meeting EHPRG, pp. 85

18. Prevorsek DC, Kavesh S (1995) Intern. J. Polymeric Mater 30: 15
19. Wawkuschewski A, Cantow HJ, Magonov SN (1994) Polym. Bull. 32: 235
20. Dijkstra DJ, Pennings AJ (1988) 19: 481
21. Dessain B, Moulaert O, Keunigs R, Bunsell AR (1992) J. Mater. Sci. 27:4515
22. Smith KJ (1990) Polym. Eng. Sci. 30: 437
23. Yamamoto T, Miyaji H, Asai K (1977) Jpn. J. Appl. Phys 16:1891
24. Amornsakchai T, Unwin AP, Ward IM, Batchelder DN (1997) Macromolecules 30:5034
25. Grubb DT, Li ZF (1992) Polymer 33:2587
26. Clough SB (1970) J. Macromol. Sci. Phys. B4:199
27. Murthy NS, Correale ST, Kavesh S (1990) Polym. Comm. 31:50
28. Smook J, Hamersma W, Pennings AJ (1984) 19:1359
29. Penning JP, De Vries AA, Pennings AJ (1993) Polym. Bull. 31:243